BRAIN
ORIGINAL ARTICLE

MerTK is a mediator of alpha-synuclein fibril uptake by human microglia

Marie-France Dorion,[1,2,3] Moein Yaqubi,[2,3] Konstantin Senkevich,[4,5] Nicholas W. Kieran,[2] Adam MacDonald,[2,3] Carol X.-Q. Chen,[1,3] Wen Luo,[1,3] Amber Wallis,[6] Irina Shlaifer,[1,3] Jeffery A. Hall,[3] Roy W. R. Dudley,[7] Ian A. Glass,[8] Birth Defects Research Laboratory,[8] Jo Anne Stratton,[2,3] Edward A. Fon,[1,3,4] Tim Bartels,[6] Jack P. Antel,[2,3] Ziv Gan-or,[4,5] Thomas M. Durcan[1,3] and Luke M. Healy[2,3]

Mer tyrosine kinase (MerTK) is a receptor tyrosine kinase that mediates non-inflammatory, homeostatic phagocytosis of diverse types of cellular debris. Highly expressed on the surface of microglial cells, MerTK is of importance in brain development, homeostasis, plasticity and disease. Yet, involvement of this receptor in the clearance of protein aggregates that accumulate with ageing and in neurodegenerative diseases has yet to be defined. The current study explored the function of MerTK in the microglial uptake of alpha-synuclein fibrils which play a causative role in the pathobiology of synucleinopathies.

Using human primary and induced pluripotent stem cell-derived microglia, the MerTK-dependence of alpha-synuclein fibril internalization was investigated *in vitro*. Relevance of this pathway in synucleinopathies was assessed through burden analysis of *MERTK* variants and analysis of MerTK expression in patient-derived cells and tissues.

Pharmacological inhibition of MerTK and siRNA-mediated *MERTK* knockdown both caused a decreased rate of alpha-synuclein fibril internalization by human microglia. Consistent with the non-inflammatory nature of MerTK-mediated phagocytosis, alpha-synuclein fibril internalization was not observed to induce secretion of pro-inflammatory cytokines such as IL-6 or TNF, and downmodulated IL-1β secretion from microglia. Burden analysis in two independent patient cohorts revealed a significant association between rare functionally deleterious *MERTK* variants and Parkinson's disease in one of the cohorts ($P = 0.002$). Despite a small upregulation in *MERTK* mRNA expression in nigral microglia from Parkinson's disease/Lewy body dementia patients compared to those from non-neurological control donors in a single-nuclei RNA-sequencing dataset ($P = 5.08 \times 10^{-21}$), no significant upregulation in MerTK protein expression was observed in human cortex and substantia nigra lysates from Lewy body dementia patients compared to controls. Taken together, our findings define a novel role for MerTK in mediating the uptake of alpha-synuclein fibrils by human microglia, with possible involvement in limiting alpha-synuclein spread in synucleinopathies such as Parkinson's disease. Upregulation of this pathway in synucleinopathies could have therapeutic values in enhancing alpha-synuclein fibril clearance in the brain.

1 Early Drug Discovery Unit, Montreal Neurological Institute-Hospital, McGill University, Montreal H3A 2B4, Canada
2 Neuroimmunology Unit, Montreal Neurological Institute-Hospital, McGill University, Montreal H3A 2B4, Canada
3 Department of Neurology and Neurosurgery, Montreal Neurological Institute-Hospital, McGill University, Montreal H3A 2B4, Canada
4 McGill Parkinson Program and Neurodegenerative Diseases Group, Montreal Neurological Institute-Hospital, McGill University, Montreal H3A 2B4, Canada
5 Department of Human Genetics, McGill University, Montreal H3A 0C7, Canada
6 UK Dementia Research Institute, University College London, London WC1E 6BT, UK

Received March 08, 2023. Revised July 26, 2023. Accepted August 29, 2023. Advance access publication September 6, 2023

7 Department of Pediatric Surgery, Division of Neurosurgery, Montreal Children's Hospital, McGill University Health Centers, Montreal H4A 3J1, Canada
8 Department of Pediatrics, University of Washington, Seattle, WA 98195, USA

Correspondence to: Thomas M. Durcan
Montreal Neurological Institute-Hospital
McGill University, 3801 Rue University
Montreal, Quebec H3A 2B4, Canada
E-mail: thomas.durcan@mcgill.ca

Correspondence may also be addressed to: Luke M. Healy
E-mail: luke.healy@mcgill.ca

Keywords: microglia; MerTK; alpha-synuclein; phagocytosis; Parkinson's disease

Introduction

Synucleinopathies are neurodegenerative disorders characterized by the intracellular accumulation of aggregated alpha-synuclein (α-syn) protein. Broadly, they are classified into multiple system atrophy and Lewy body diseases that include Parkinson's disease and Lewy body dementia. The neuronal accumulation of α-syn in the form of Lewy bodies and its role in neurodegenerative processes have been extensively studied. Duplication or triplication of the genetic locus encoding α-syn (*SNCA*) have been identified to cause autosomal dominant Parkinson's disease,[1] implying that accumulation of excess α-syn is sufficient to trigger the disease process. Current evidence supports the notion that the initiation of α-syn aggregation, either in the CNS or peripheral tissues, can then propagate in a prion-like manner into the brain, where it induces neuronal dysfunction and degeneration.[2-7] Accordingly, injection of recombinant α-syn preformed fibrils (PFFs) into mice leads to the development of Lewy body-like pathologies, neuronal loss and behavioural deficits.[8] *In vitro*, seeding of neurons with α-syn PFFs also results in the formation of Lewy body-like inclusions and dysregulation of cellular processes.[9,10]

Strategies to prevent cell-to-cell spread of α-syn have been proposed as potential therapies to prevent neurodegeneration in synucleinopathies.[11] Mechanisms involved in α-syn endocytosis are being actively explored, with differential internalization mechanisms observed across brain cell types. For instance, heparan sulfate proteoglycans have been identified as mediators of α-syn PFF internalization by neurons but not microglia.[12] Microglia, as professional phagocytes residing in the brain, can internalize and degrade α-syn fibrils at a higher rate than other cells,[13-15] making them a particularly promising cell type that can be targeted in the development of novel therapeutics to promote α-syn clearance. The majority of microglia studies investigating α-syn internalization processes to date have been carried out using murine microglia or the murine microglia-like cell line BV2 and have contributed to the identification of a variety of cell surface proteins that interact with human α-syn, including toll-like receptors (TLRs) and cluster of differentiation 36.[16-20] Since human and murine microglia are inherently different in their genome, transcriptome and aspects of their function,[21-24] it is unclear whether the same receptors and mechanisms participate in the uptake of α-syn by human microglia.

In a previous study comparing the impact of culture media formulation on microglia phagocytic activities, we observed a correlation between α-syn fibril and myelin debris uptake activities[25] suggestive of a common mechanism of internalization for these substrates. Both α-syn fibril and myelin debris uptake activities also correlated with the expression level of Mer tyrosine kinase (MerTK), a microglial surface receptor kinase with known roles in myelin phagocytosis.[26]

TYRO3, AXL and MerTK constitute the 'TAM' family of homologous receptor tyrosine kinases with pleiotropic functions. AXL and MerTK are particularly known for their roles in the phagocytosis of apoptotic cells,[27] myelin debris,[26] synapses[28] and photoreceptor outer segments.[29,30] Tethering of phagocytic targets to TAM receptors occurs through the binding of secreted bridging molecules—growth arrest-specific 6 (GAS6) and protein S1 (PROS1)—with high affinity for phosphatidylserine moieties exposed on the membranes of dead cells.[31] Binding of GAS6/PROS1 to TAM receptors triggers activation of the cytoplasmic kinase domain, autophosphorylation and downstream signalling that induces the cytoskeletal remodelling required for phagocytosis.[31] This process is immunologically silent and suppresses the inflammatory activation of myeloid cells during homeostatic phagocytosis.[31,32]

High expression of MerTK, as well as its activating ligands GAS6 and PROS1, is a characteristic feature of microglia that distinguishes them from other myeloid populations.[33] The present study aimed to investigate the role of MerTK in α-syn fibril uptake by human primary and induced pluripotent stem cell-derived microglia (iMGL). The relevance of this process in synucleinopathies was evaluated through rare variant burden analysis of *MERTK* in Parkinson's disease and assessment of MerTK expression in patient-derived brain materials. Taken together, we show that α-syn fibril uptake by human microglia is largely MerTK-dependent. Lack of MerTK upregulation accompanying α-syn accumulation in the human brain and genetic associations between rare *MERTK* variants and Parkinson's disease suggest MerTK as a potential therapeutic target to enhance α-syn fibril clearance by microglia in synucleinopathies.

Materials and methods

Ethical approval

Use of all human materials was approved by the McGill University Health Centre Research Ethics Board under project no. 1989-178 for human brain tissues and 2019-5374 for induced pluripotent stem cells (iPSCs).

Microglia isolation and culture

Cortical tissues from 2- to 68-year-old female and male epilepsy patients were obtained from the Montreal Neurological Institute, Montreal, Canada (adult donors), and the Montreal Children's Hospital, Montreal, Canada (paediatric donors), with written consent and under approval from local ethics boards. Tissue samples were aspirated into ultrasonic surgical aspirator bags (CUSA®) from the surgical 'corridor' away from the site of suspected epileptic foci. Materials were comprised predominantly of white matter tissue. Focal or diffused pathology were excluded as much as possible during the operative procedure and retrospective histological analyses. Samples were excluded from the study when brain tumours were discovered to be associated with epileptic seizures. Second trimester fetal cerebrum tissues were obtained from Centre Hospitalier Universitaire Sainte-Justine, Montreal, Canada, or from the Birth Defects Research Laboratory, University of Washington, Seattle, USA, with maternal written consent and under approval from local ethics boards. Demographic information about the donors is included in Supplementary Table 1. Isolation of glial cells was carried out as previously described[34] through mechanical and chemical digestion, followed by Percoll® (Sigma-Aldrich) gradient centrifugation (postnatal tissue) or not (fetal tissue). Microglia were further purified by taking advantage of the differential adhesive properties of the glial cells. This resulted in a culture purity of ~97% as assessed by PU.1 immunostaining (Supplementary Fig. 1A and B). *Ex vivo* human postnatal microglia (hMGL) were prepared by magnetic activated bead sorting of CD11b+ cells immediately after tissue processing as previously described.[25] HMGL were maintained *in vitro* in microglia growth medium composed of Dulbecco's modified Eagle's medium (DMEM)/F12 (Thermo Fisher Scientific), 1% GlutaMAX™ (Thermo Fisher Scientific), 1% non-essential amino acids (Thermo Fisher Scientific), 1% penicillin/streptomycin (P/S; Thermo Fisher Scientific), 2× insulin-transferrin-selenium (Thermo Fisher Scientific), 2× B27 (Thermo Fisher Scientific), 0.5× N2 (Thermo Fisher Scientific), 400 μM monothioglycerol (Sigma Aldrich) and 5% fetal bovine serum (FBS; Wisent Bioproducts), which was previously shown to promote high phagocytic activity and MerTK expression.[25] When indicated, hMGL were polarized by treating them with 20 ng/ml interferon gamma (IFNγ; Peprotech) and 100 ng/ml Pam_3CSK_4 (Invivogen) for 48 h or left unpolarized. Fetal microglia (fMGL) were cultured in DMEM (Sigma-Aldrich) supplemented with 1% GlutaMAX™, 1% P/S and 5% FBS. Cells were maintained at 37°C under a 5% CO_2 atmosphere.

Generation of iMGL

A number of iPSC lines were used in our study to ensure reproducibility of our findings across lines obtained from different sources: DYR0100 (American Type Cell Collection), KYOU-DXR0109B (American Type Cell Collection), GM25256 (Coriell Institute) and 3450 (generated in-house as previously described[35]). All iPSCs were from individuals with no known neurological diseases. Donor information and reprogramming methods are indicated in Supplementary Table 2. Differentiation of iPSCs into iMGL was carried out following a previously established protocol.[36] Briefly, haematopoietic progenitor cells were generated from iPSCs using a STEMdiff Hematopoietic kit (STEMCELL Technologies) and cultured in microglia growth medium supplemented with 100 ng/ml interleukin-34, 50 ng/ml tumour growth factor-beta 1 and 25 ng/ml macrophage colony-stimulating factor (Peprotech) for 25 days, following which 100 ng/ml cluster of differentiation 200 (Abcam) and C-X3-C motif chemokine ligand 1 (Peprotech) were also added to the culture. Cells were maintained at 37°C under a 5% CO_2 atmosphere throughout the protocol. The final culture had a purity of 99% as assessed by PU.1 immunostaining (Supplementary Fig. 1A and B). IMGL expressed a variety of microglia markers at higher levels compared to peripheral blood mononuclear cell-derived macrophages (Supplementary Fig. 1C) or iPSCs.[25]

Peripheral blood mononuclear cell-derived macrophages

Peripheral blood mononuclear cell-derived macrophages (PBMCs) were isolated from whole blood of healthy individuals (20-year-old female, 24-year-old male, 29-year-old female and 32-year-old male) by Ficoll gradient centrifugation. Monocytes were then collected through magnetic activated bead sorting of CD11b + cells and cultured at a density of $5–10 \times 10^5$ cells/cm^2 (Day 0) in RPMI-1640 (Thermo Fisher Scientific) with 10% FBS, 1% P/S, 1% GlutaMAX™ and 30 ng/ml M-CSF (Peprotech). Cells were matured for 8 days, with media supplementation on Day 4 and Day 7.

RNA-sequencing

RNA-sequencing (RNAseq) data were obtained from an earlier study.[25] Quality control of the RNA samples, library preparation and RNAseq were performed by Genome Quebec, Montreal, Canada. The library was generated using a NEBNext® Single Cell/Low Input RNA Library Prep kit (New England Biolabs). RNAseq was performed using an Illumina NovaSeq 6000. The Canadian Center for Computational Genomics' pipeline GenPipes[37] was used to align the raw files and quantify the read counts.

Western blotting

Cells were lysed on ice in a lysis buffer composed of 150 mM NaCl, 50 mM Tris-HCl pH 7.4, 1% Nonidet P-40, 0.1% sodium dodecyl sulfate (SDS) and 5 mM EDTA with protease and phosphatase inhibitors (Thermo Fisher Scientific). Cell lysates were centrifuged at 500*g* for 30 min at 4°C to remove cellular debris. Proteins (25 μg/lane) were separated on SDS-polyacrylamide gels and transferred to polyvinylidene difluoride membranes (Bio-Rad Laboratories). For the detection of α-syn, membranes were fixed in 4% paraformaldehyde solution as previously described.[38] Membranes were immunoblotted for AXL (AF154 R&D Systems at 1:500), MerTK (ab52968, Abcam at 1:500), phosphorylated MerTK (p186-749, Phosphosolutions at 1:1000), α-syn (ab138501, Abcam 1:5000), S129-phosphorylated α-syn (ab51253, Abcam 1:1000), CSF1R (MAB3291, R&D systems; 1:250) and glyceraldehyde 3-phosphate dehydrogenase (GAPDH; G8795, Sigma Aldrich at 1:5000) overnight at 4°C, and then with horse radish peroxidase-linked secondary antibodies (1:10 000; Jackson Laboratory) for 1 h. Bands were detected by enhanced chemiluminescence with Clarity Max ECL substrates (Bio-Rad Laboratories) using a ChemiDoc Imaging System (Bio-Rad Laboratories). Image analysis was performed using ImageLab 6.0.1 software (Bio-Rad Laboratories).

Preparation of α-syn preformed fibrils

PFFs of α-syn were generated as previously described[39,40] with slight modifications. Briefly, glutathione-S-transferase (GST)-tagged

human recombinant α-syn were expressed and isolated from *Escherichia coli*. The GST tag was removed and purified α-syn monomers were subjected to endotoxin removal using Pierce™ High-Capacity Endotoxin Removal Resin (Thermo Fisher Scientific) to achieve endotoxin levels <0.3 EU/mg. α-Syn monomers were aggregated on a shaker for 5 days with constant shaking at 1000 rpm and 37°C. Resulting PFFs were subjected to 40–80 cycles of sonication (30 s on/30 s off) using a Zetasizer Nano (Malvern Panalytical) to achieve ∼50–100 nm sizes. Sizes and morphology of PFFs were monitored by electron microscopy and dynamic light scattering (Supplementary Fig. 2A and B). A thioflavin T assay was used to confirm the presence of beta-sheet structure (Supplementary Fig. 2C). All data were validated using α-syn PFFs from at least two different batches.

Proximity ligation assay

Cells in suspension were incubated with vehicle or α-syn PFFs (1 μM) on ice for 30 min to allow binding, but not internalization, of α-syn PFFs. Unbound α-syn PFFs were washed away, and cells were fixed in 2% formaldehyde solution on ice for 30 min. A proximity ligation assay (PLA) was performed using a Duolink® FlowPLA kit following the manufacturer's recommendations. The following primary antibodies were used: rabbit anti-α-syn (1:200; ab138501, Abcam), mouse anti-α-syn (1:200; ab1903, Abcam), mouse anti-MerTK (1:1000; 367602, Biolegend) and mouse anti-AXL (1:1000; MAB154, R&D Systems). Antibodies against α-syn were tested on vehicle versus α-syn PFF-treated cells to ensure that they selectively bound to exogenous but not endogenous α-syn (Supplementary Fig. 3). Data acquisition was done on an Attune™ Nxt Flow Cytometer and analysis was done using FlowJo™ software.

Uptake assay

Human α-syn PFFs, myelin debris[26] and immunoglobulin G-opsonized red blood cells[41] (IgG-RBCs) were labelled with pHRodo Green™ STP ester (Thermo Fisher Scientific) and used at the following respective concentrations, which were determined to be non-saturating: 1 μM, 15 μg/ml and 50 000 cells/ml, respectively. Cells were incubated with the labelled substrates for 2 h and then counterstained with Hoechst 33342 (5 μg/ml). Total green fluorescence intensity per cell was quantified using a CellInsight CX5 High Content Screening Platform (Thermo Fisher Scientific). All conditions were assessed in triplicate. Background/autofluorescence subtraction was carried out on all data except those presented in Fig. 1F and H, using fluorescence intensity quantified in unchallenged cells. Internalization of Alexa Fluor 488-conjugated human α-syn PFFs (1 μM) and epidermal growth factor (EGF; 4 μg/ml; Thermo Fisher Scientific) were assessed similarly, except cells were washed with 0.4% trypan blue solution to quench extracellular fluorescence. When indicated, cells were pretreated for 1 h with non-cytotoxic concentrations of UNC2025 (3 μM; Cayman Chemical) or cytochalasin D (1 μM; Sigma Aldrich). At the concentration of 3 μM, UNC2025 inhibited the autophosphorylation of MerTK in iMGL induced by GAS6 + H_2O_2 treatment (Supplementary Fig. 4).

RNA interference

Cells were transfected with siGENOME RISC-Free Control (siCON) or ON-TARGETplus small interfering RNA (siRNA) pools against *MERTK* (siMERTK, at 20 nM) and/or *AXL* (siAXL, at 10 nM) (Horizon Discovery) using Lipofectamine™ RNAiMAX (Thermo Fisher Scientific). The manufacturers' protocols were followed. When necessary, siCON was used to equilibrate the total amount of siRNA received by cells across experimental conditions.

Flow cytometry

Cells were blocked with Human TrueStain FcX and TrueStain Monocyte Blocker (Biolegend) and stained with the following antibodies: anti-AXL clone #108724 and anti-MERTK clone #125518 (R&D Systems). Appropriate forward and side scatter profiles were used to exclude debris and doublets from the analysis. Dead cells were excluded based on LIVE/DEAD™ Fixable Aqua (Thermo Fisher Scientific) staining. Readings were done on an Attune™ Nxt Flow Cytometer and analysed/visualized using FlowJo™ software.

Cell viability

Cell viability was assessed by propidium iodide (PI; Thermo Fisher Scientific) staining unless otherwise specified. Cells were stained in phosphate buffered saline containing 1 μg/ml PI and 5 μg/ml Hoechst 33342 (Thermo Fisher Scientific) and the average number of PI- live cells per condition was determined using a CellInsight CX5 High Content Screening Platform. All conditions were assessed in triplicate. Viability was calculated as follows:

$$Viability_{control}\ (\%) = 100 \times \frac{\#viable\ cells_{control}}{\#viable\ cells_{control}} \quad (1)$$

$$Viability_{experimental}(\%) = 100 \times \frac{\#viable\ cells_{experimental}}{\#viable\ cells_{control}} \quad (2)$$

where

$$\#viable\ cells_{control} = total\ nuclei\ count_{control} - PI\ count_{control} \quad (3)$$

$$\#viable\ cells_{experimental} = total\ nuclei\ count_{experimental} - PI\ count_{experimental} \quad (4)$$

Quantitative reverse transcription PCR

A RNeasy mini kit (Qiagen) was used to extract RNA. Reverse transcription was performed using Moloney murine leukemia virus reverse transcriptase (Thermo Fisher Scientific) and real-time PCR was performed using TaqMan assays (Thermo Fisher Scientific) on a QuantStudio™ 5 real-time PCR system (Thermo Fisher Scientific). The $2^{-\Delta Ct}$ method was used to analyse the data using *GAPDH* and tyrosine 3-monooxygenase/tryptophan 5-monooxygenase activation protein zeta (*YWHAZ*) as controls.

Measurement of cytokine secretion

Concentrations of interleukin-1beta (IL-1β), interleukin-6 (IL-6), interleukin-10 (IL-10) and tumor necrosis factor (TNF) in cell supernatants were measured using the Human Inflammatory Cytokine Cytometric Bead Array Kit (BD Biosciences). Readings were done on an Attune™ Nxt Flow Cytometer.

Burden analysis of rare variants

Rare variant analysis was performed in the UK Biobank (UKBB) cohort, composed of 602 Parkinson's disease patients and 15 000 randomly sampled controls, and the Accelerating Medicines

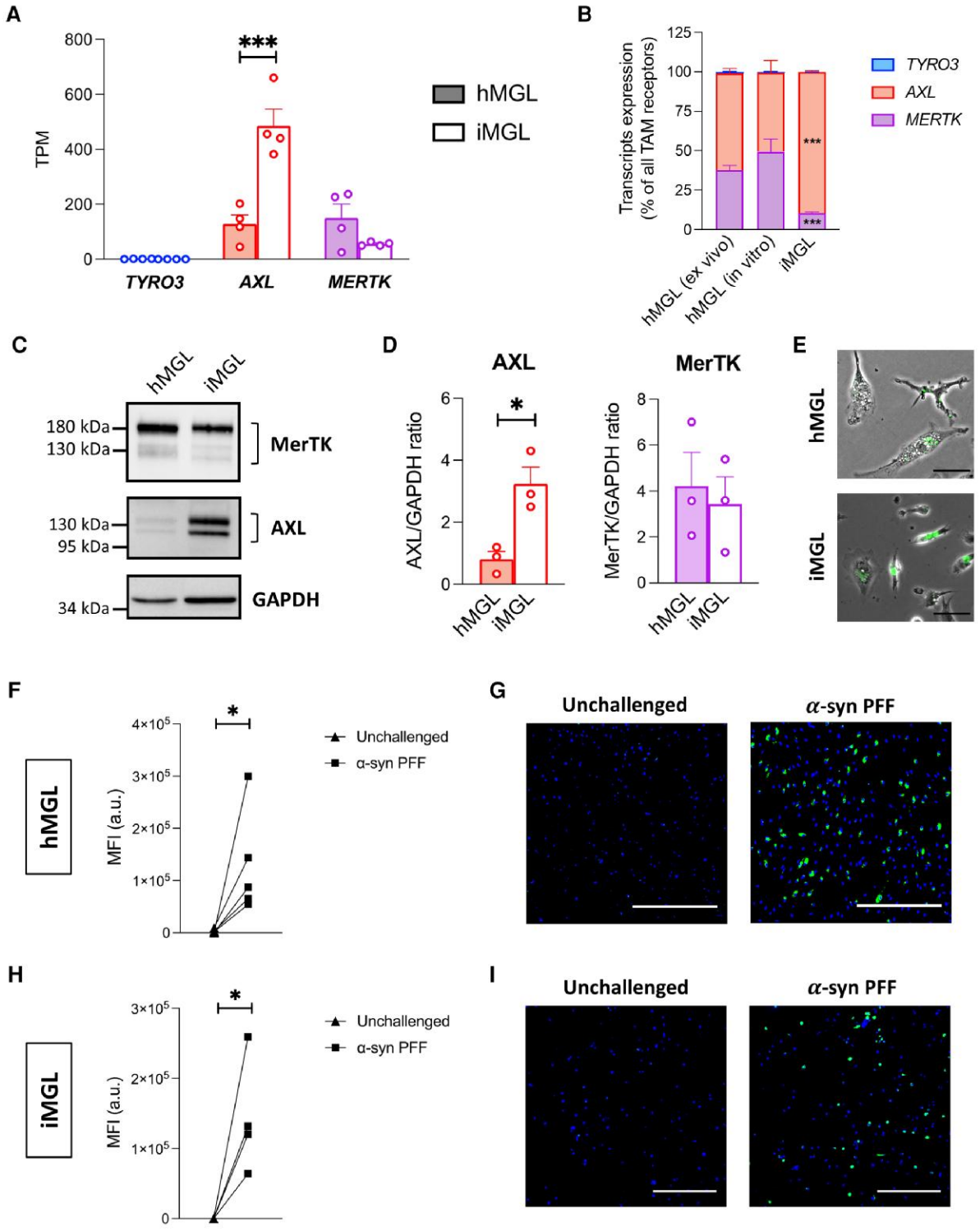

Figure 1 TAM receptors expression and α-synuclein preformed fibril uptake by human microglia. All human primary microglia (hMGL) data are from *in vitro* hMGL, unless otherwise specified. (**A** and **B**) RNA-sequencing (RNAseq) assessment of *TYRO3*, *AXL* and *MERTK* expression in hMGL and induced pluripotent stem cell-derived microglia (iMGL). A one-way ANOVA with Sidak's *post hoc* test was performed for pairwise comparisons between hMGL and iMGL in **A**. TPM = transcripts per million. Mean ± SEM of $n = 4$; $^{***}P < 0.001$. A two-way ANOVA with Dunnett's *post hoc* test was performed to compare *in vitro* hMGL and iMGL to *ex vivo* hMGL in **B**. Mean ± SEM of $n = 4$; $^{***}P < 0.001$ versus *ex vivo* hMGL. (**C**) Western blot of MerTK, AXL and GAPDH. (**D**) Quantification of AXL and MerTK expression using GAPDH as a loading control. *t*-tests were performed. Mean ± SEM of $n = 3$; $^{*}P < 0.05$. (**E–I**) hMGL and iMGL were challenged with pHrodo™ Green-labelled α-synuclein (α-syn) preformed fibrils (PFFs) for 2 h. (**E**) Merged phase contrast and green fluorescence images. Scale bar = 50 μm. (**F**) Quantification of mean green fluorescence intensity (MFI) in hMGL culture. A paired *t*-test was performed; $n = 5$; $^{*}P < 0.05$; a.u. = arbitrary unit. (**G**) Representative fluorescence images of hMGL counterstained with Hoechst 33342 (blue). Scale bar = 500 μm. (**H**) Quantification of MFI in iMGL culture. A paired *t*-test was performed; $n = 4$; $^{*}P < 0.05$; a.u. = arbitrary unit. (**I**) Representative fluorescence images of iMGL counterstained with Hoechst 33342 (blue). Scale bar = 300 μm.

Partnership-Parkinson Disease (AMP-PD) initiative cohort, composed of 2341 Parkinson's disease patients and 3486 controls. All Parkinson's disease patients were diagnosed according to either the UK Brain Bank criteria[42] or the Movement Disorders Society criteria.[43] Only individuals with European ancestry were included. For the UKBB cohort, whole-exome sequencing data were used. Quality control was performed both at the individual and variant levels using Genome Analysis Toolkit (GATK, v3.8) and plink, with a minimum depth of coverage = 10 and GQ = 20 as described previously.[44] For the AMP-PD cohort, all available whole-genome sequencing data were used for which the quality control processes at the individual and variant levels have previously been described (https://amp-pd.org/whole-genome-data). Associations between variants and Parkinson's disease were tested using the optimized sequence Kernel association test (SKAT-O).[45] Variants were categorized into (i) rare (minor allele frequency <1%) non-synonymous variants; (ii) functional variants (nonsynonymous, stop/frameshift and splicing); and (iii) variants with a combined annotation dependent depletion (CADD) score of ≥20, representing the top 1% of potentially deleterious variants. A meta-analysis of the two cohorts was run using the metaSKAT package.[46]

Analysis of single-nuclei RNA-sequencing data

Single-nuclei RNAseq data for human substantia nigra were obtained from Kamath *et al.*[47] and accessed through GEO:178265. The dataset included eight non-neurological control donors, seven Parkinson's disease patients and three Lewy body dementia patients. All patients were pathologically confirmed to present moderate to prominent loss of pigmentation in the substantia nigra.[47] The microglia population was subtracted from the main object using metadata information provided by the authors at the Broad Institute Single Cell Portal https://singlecell.broadinstitute.org/single_cell/study/SCP1768/. The subtracted microglia population was subjected to the standard Seurat pipeline for dimensionality reduction, gene expression normalization, clustering and differential expression analysis. Twenty clusters expressing microglia canonical markers were identified (Supplementary Fig. 5), among which Clusters 8, 12, 16 and 17 showed enrichment in stress response genes typically associated with tissue dissociation procedures (Supplementary Table 3). Those clusters, along with Cluster 11 with macrophage marker expression (Supplementary Table 3), were removed from further analysis. Differentially expressed genes (DEGs) between Parkinson's disease/Lewy body dementia and control microglia were identified using $|\log_2(\text{fold change})| > 0.25$ and adjusted *P*-value < 0.05 as cut-offs. Microglia from control, Parkinson's disease and Lewy body dementia samples were integrated using the canonical correlation analysis (CCA) of the Seurat pipeline. Microglia clusters identified post-integration were used to generate Supplementary Figs 11 and 12.

Preparation of human brain tissue lysates

Human substantia nigra tissues were from the Netherlands Brain Bank (NBB), Netherlands Institute for Neuroscience, Amsterdam, Netherlands (open access: www.brainbank.nl), and derived from nine Lewy body dementia patients and nine control donors. All materials were collected from donors for or from whom a written informed consent for a brain autopsy and the use of the material and clinical information for research purposes had been obtained by the NBB. Since availability of substantia nigra from non-neurological controls was limited, substantia nigra from control donors presenting non-synucleinopathy neurological disorders sparing the substantia nigra were used. All control donors had normal appearing, pigmented substantia nigra. Clinicopathological information about the donors is presented in Supplementary Table 4. Detailed clinicopathological information is available upon request. Human cortex tissues were from the Mayo Clinic Brain Bank, Jacksonville, USA, and derived from five Lewy body dementia patients and five control donors devoid of Lewy body disease, from or for whom a written informed consent for a brain autopsy and the use of the material and clinical information for research purposes had been obtained. Clinicopathological information about the donors is presented in Supplementary Table 5.

Tissues were dounce-homogenized in Tris-buffered saline with protease and phosphatase inhibitors. Samples were further diluted in Tris-buffered saline with 5% SDS, 8 M urea, protease and phosphatase inhibitors for protein extraction. Insoluble materials were removed by centrifugation at 13 000*g* for 10 min.

Statistical analyses

Statistical analyses were performed using GraphPad Prism 9.0 software. A *t*-test was used to compare the mean of two groups of data. A one-way ANOVA was used to compare the mean of three or more groups of data. When the assumptions of a *t*-test (normal distribution) or a one-way ANOVA (normal distribution and homoscedasticity) were not met, a Mann–Whitney or Kruskal–Wallis test was used instead, respectively. Paired or repeated measure analyses were performed for experiments involving hMGL from the same individuals or iMGL from the same differentiation batches subjected to two or more treatment conditions. *P*-values were adjusted using appropriate *post hoc* tests in the case of multiple comparisons. Mean and standard error of the mean (SEM) of biological replicates (*n*) are plotted in all graphs unless otherwise indicated. A $P < 0.05$ was considered statistically significant. HMGL obtained from independent donors and iMGL generated at different points in time were considered biological replicates.

Results

HMGL and iMGL express MerTK and internalize α-syn preformed fibrils

We first aimed to assess the MerTK-dependence of α-syn PFF uptake by human microglia. Given the limited access to hMGL, the potential of iMGL as an alternative model to investigate the role of MerTK in α-syn PFF uptake was evaluated. RNAseq and western blotting of TAM receptor expression revealed that both AXL and MerTK are expressed in hMGL and iMGL (Fig. 1A–D). Interestingly, AXL expression was significantly higher in iMGL compared to hMGL, whereas MerTK expression was similar between both cell types (Fig. 1A–D). As expected, *TYRO3* expression was low in both models (Fig. 1A and B). Microglia undergo a major transcriptomic change from their freshly isolated state (*ex vivo*) to a cultured state (*in vitro*).[23,25] RNAseq assessment of TAM receptor expression revealed a similar *MERTK:AXL* expression ratio between *ex vivo* and *in vitro* hMGL, whereas this ratio was lower in iMGL (Fig. 1B). This suggests the relative expression profile of TAM receptors in *in vitro* hMGL is representative of their native profile, whereas the TAM receptor expression profile in iMGL is distinct. Given these results, subsequent experiments were carried out in iMGL, with validation of key findings in hMGL.

pHrodo™ dyes are fluorogenic dyes that fluoresce when present in an acidic milieu such as phagosomes and lysosomes; and they have previously been demonstrated to be useful tools for quantifying the rate of phagocytosis.[26,48] Following incubation of iMGL with pHrodo™ Green-labelled α-syn PFFs, a dose-dependent and time-dependent increase in green fluorescence intensity per cell was quantified (Supplementary Fig. 6A and B). A concentration of 1 μM was non-saturating at the 2-h time point (Supplementary Fig. 6A and B) and resulted in readily quantifiable fluorescence intensity in both hMGL (Fig. 1E–G) and iMGL cultures (Fig. 1E, H and I).

α-Syn preformed fibrils bound on microglia cell surface are in close proximity to MerTK

PLA is a highly sensitive and specific method of assessing interactions between two proteins. A pair of antibodies raised in two different species are used to detect close proximity (<40 nm) of their respective target proteins in cellular systems.[49] IMGL were incubated on ice with α-syn PFFs, and flow cytometry-based PLA was performed to assess the interactions between α-syn PFFs and MerTK on cell surfaces. As a positive control, interactions between α-syn proteins were shown to emit high PLA signals when two different antibodies against α-syn were used, confirming α-syn/α-syn interactions within fibrils (Fig. 2A). A positive PLA signal was also detected when interaction between α-syn and MerTK was assessed (Fig. 2A and B). In contrast, signal was minimal when interaction between α-syn and AXL was measured (Fig. 2A). Overall, these data demonstrate that α-syn PFFs bound to the cell surface are in close proximity to MerTK, suggestive of an interaction between α-syn PFFs and MerTK prior to their internalization.

Pharmacological inhibition of MerTK results in decreased α-syn preformed fibrils uptake by microglia

The selective MerTK inhibitor UNC2025[50] was used to investigate the involvement of MerTK in α-syn fibril internalization by microglia. A 1-h pretreatment with UNC2025 reduced iMGL uptake of pHrodo™ Green-labelled α-syn PFFs by ~79% (Fig. 3A–C). UNC2025 also decreased pHrodo™ Green-labelled myelin uptake as previously described,[26] but had no effect on pHrodo™ Green-labelled IgG-RBC uptake, a process mediated by Fc gamma receptors and thus independent of MerTK[27,51] (Fig. 3A–C). In contrast, the actin polymerization inhibitor cytochalasin D non-selectively inhibited the internalization of all three substrates (Fig. 3A–C). UNC2025 also decreased hMGL uptake of pHrodo™ Green-labelled α-syn PFFs by ~79% (Fig. 3D and E), providing validation that MerTK kinase activity is essential for the internalization of α-syn fibrils by hMGL.

To ensure that results were not influenced by the use of a pH-sensitive dye, additional tests were performed with Alexa Fluor 488-labelled α-syn PFFs. Similar to findings with pHrodo™ Green-labelled α-syn PFFs, UNC2025 also decreased the internalization of Alexa Fluor 488-labelled α-syn PFFs by iMGL (Supplementary Fig. 7A and B), confirming that MerTK appears to mediate the internalization of α-syn PFFs regardless of the conjugated dyes. UNC2025 did not affect the internalization of Alexa Fluor 488-labelled EGF, which is known to be mediated by epidermal growth factor receptors[52] (EGFRs; Supplementary Fig. 7A and B). All subsequent uptake assays were performed using pHrodo™ Green-labelled α-syn PFFs.

MERTK knockdown results in decreased α-syn preformed fibril uptake by microglia

Small-interfering RNA-mediated knockdown experiments were next carried out to confirm that our earlier findings were a consequence of MerTK inhibition and not an off-target effect of UNC2025 on other tyrosine kinases. IMGL were transfected with siRNAs against *AXL* and/or *MERTK* and replated for the assessment of α-syn PFF uptake. siAXL and siMERTK significantly decreased the respective surface expression of AXL and MerTK on live iMGL after 48 h (Fig. 4A). Knockdown of *AXL* had no marked impact on α-syn PFF internalization by iMGL, unlike *MERTK* knockdown, which resulted in a ~71% decrease in internalization (Fig. 4B and C). Knockdown of both *AXL* and *MERTK* together did not further affect α-syn PFF uptake compared to *MERTK* knockdown alone (Fig. 4B and C). As postnatal hMGL are difficult to transfect, cells from fetal sources were used to validate the effect of *MERTK* knockdown on α-syn fibril internalization by human microglia. fMGL expressed MerTK and AXL at similar levels to hMGL (Supplementary Fig. 8A–C), and UNC2025 decreased their uptake of α-syn PFFs by ~64% (Supplementary Fig. 8D and E). *AXL* knockdown did not affect α-syn PFF uptake by fMGL, whereas *MERTK* knockdown did (by ~56%; Fig. 4D–F). Neither *AXL* nor *MERTK* knockdown affected fMGL viability (Fig. 4G), ruling out the possibility that a viability effect was downregulating PFF internalization. Altogether, these findings implied that MerTK but not AXL is essential for α-syn fibril uptake by human microglia.

Previously, it has been shown that combined stimulation of microglia with IFNγ and a TLR agonist, the so-called 'M1' polarization, results in a pro-inflammatory phenotype characterized by decreased expression of MerTK and lower internalization of myelin debris.[26] Polarization of hMGL with IFNγ and the TLR2/1 agonist Pam_3CSK_4 was confirmed to increase the expression of inflammatory markers such as human leukocyte antigen-DR (*HLA-DR*), *TNF* and C-X-C motif chemokine ligand 10 (*CXCL10*), and to decrease *IL10* expression compared to the unpolarized state (Supplementary Fig. 9A). Expression of genes encoding MerTK and its activating ligands GAS6 and PROS1 were decreased in cells polarized with IFNγ and Pam_3CSK_4 whereas AXL expression was unchanged (Supplementary Fig. 9A). This decreased expression of *MERTK*, *GAS6* and *PROS1* was associated with significantly lower uptake of α-syn PFFs (Supplementary Fig. 9B and C), further supporting the notion that MerTK alone, not AXL, mediates α-syn fibril uptake by human microglia.

MerTK-mediated α-syn preformed fibril uptake has an immunomodulatory effect on microglia

Phagocytic processes involving MerTK are known to be non-inflammatory and can even induce immunosuppression.[53] With pharmacological and knockdown assays pointing towards MerTK being a central mediator of α-syn fibril uptake, the effects of α-syn PFFs on immune pathways was investigated. Pam_3CSK_4 significantly increased the secretion of IL-6 and TNF by iMGL, confirming that these cells can be activated to secrete cytokines (Fig. 5A). Consistent with the idea that MerTK-mediated phagocytosis is immunologically silent, a 24-h treatment with α-syn PFFs did not result in increased iMGL secretion of IL-6, TNF, IL-10 or IL-1β (Fig. 5A). Interestingly, a modest but statistically significant decrease in the secretion of those cytokines was observed following α-syn PFF treatment (Fig. 5B), indicative of an immunomodulatory effect. The α-syn PFF-induced decrease in IL-6, TNF and IL-1β was prevented by a 1-h pretreatment of iMGL with UNC2025 or cytochalasin D

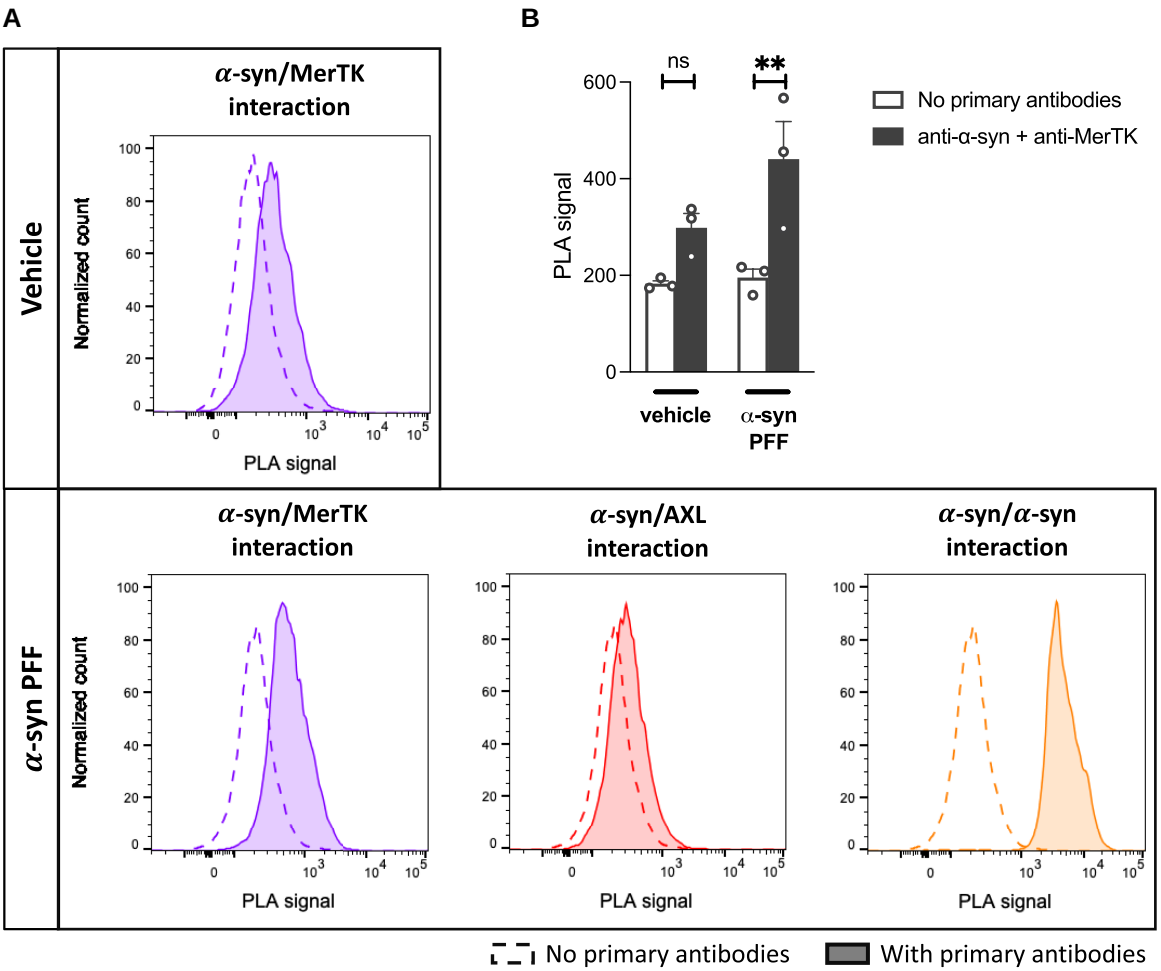

Figure 2 Interaction between α-synuclein preformed fibrils and MerTK. Induced pluripotent stem cell-derived microglia (iMGL) were incubated with α-synuclein (α-syn) preformed fibrils (PFFs) or vehicle on ice for 30 min and a proximity ligation assay (PLA) was performed. (**A**) Representative flow cytometry plots. (**B**) Quantification of the PLA signals. A repeated measure one-way ANOVA was performed followed by Sidak's *post hoc* test. Mean ± SEM of $n = 3$; $^{**}P < 0.01$.

(Fig. 5B), suggesting that this immunomodulatory effect is dependent on MerTK-mediated α-syn PFF internalization. The decrease in IL-10 was not prevented by UNC2025 or cytochalasin D pretreatment (Fig. 5B), suggesting that this effect of α-syn PFFs is independent from their internalization. Treatment of hMGL with α-syn PFFs also did not elicit an increase in IL-6, TNF, IL-10 or IL-1β secretion (Fig. 5C). IL-1β secretion by hMGL was significantly inhibited by α-syn PFFs (Fig. 5C). In hMGL, α-syn PFFs were also found to inhibit lipopolysaccharide (LPS)-induced IL-1β secretion (Fig. 5D).

Expression of a wider range of cytokines was assessed in iMGL by qRT-PCR following 3 h, 1 day and 7 days of α-syn exposure. In contrast to Pam_3CSK_4, neither the monomeric nor fibrillar forms of α-syn increased the transcriptional expression of cytokines (Supplementary Fig. 10). To summarize, α-syn did not induce an inflammatory response of human microglia similar to that triggered by TLR stimulation.

Rare deleterious *MERTK* variants are associated with Parkinson's disease

To further examine the potential role of MerTK-mediated phagocytosis in synucleinopathies, genetic associations between rare *MERTK* variants and Parkinson's disease were investigated by burden analysis in two independent patient cohorts: UKBB and AMP-PD. A significant association between *MERTK* variants with CADD score ≥20 (representing the top 1% of potentially deleterious variants) and Parkinson's disease was found in the UKBB cohort ($P = 0.002$; Table 1). However, this association was not observed in the AMP-PD cohort or following a meta-analysis of both cohorts (Table 1). This could be a result of specific variants associated with Parkinson's disease being underrepresented in the AMP-PD cohort. No significant associations were found between *AXL* variants and Parkinson's disease (Table 1). Overall, these results suggest that some rare, functionally deleterious *MERTK* variants may be associated with Parkinson's disease, however these findings require additional replications.

MerTK protein expression is unaltered in brain lysates of Lewy body dementia patients

Following the observation that rare genetic variants of *MERTK* are potentially associated with Parkinson's disease, the possibility that the MerTK pathway is dysregulated in the Parkinson's disease substantia nigra was investigated using a previously published post-mortem snRNAseq dataset.[47] DEG analysis of microglia from Parkinson's disease ($n = 7$) or Lewy body dementia ($n = 3$) substantia

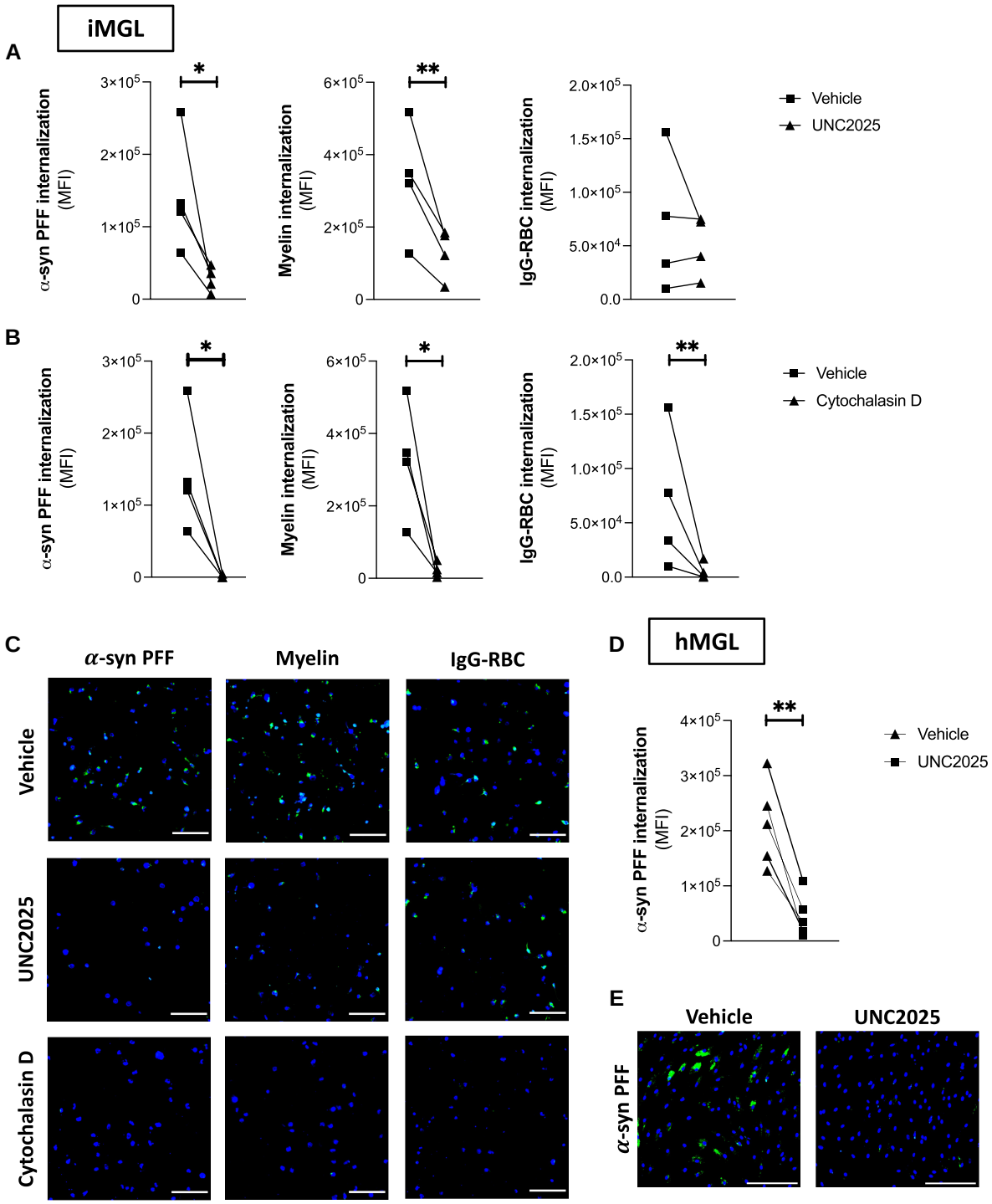

Figure 3 Effect of UNC2025 on microglial uptake of α-synuclein preformed fibrils. Microglia were pretreated with vehicle, UNC2025 (3 μm) or cytochalasin D (1 μm) for 1 h, then challenged with pHrodo™ Green-labelled α-synuclein (α-syn) preformed fibrils (PFFs), myelin debris or IgG-opsonized red blood cells (IgG-RBC) for 2 h. (**A** and **B**) Quantification of mean green fluorescence intensity (MFI) in induced pluripotent stem cell-derived microglia (iMGL) culture. Paired *t*-tests were performed; $n = 4$; $^{*}P < 0.05$, $^{**}P < 0.01$. (**C**) Representative images of iMGL counterstained with Hoechst 33342 (blue). Scale bar = 150 μm. (**D**) Quantification of mean green fluorescence intensity (MFI) in human primary microglia (hMGL) culture. A paired *t*-test was performed; $n = 5$; $^{**}P < 0.01$. (**E**) Representative images of hMGL counterstained with Hoechst 33342 (blue). Scale bar = 200 μm.

nigra tissues compared to those of non-neurological controls ($n = 8$) revealed a decrease in expression of the homeostatic markers C-X3-C motif chemokine receptor 1 (*CX3CR1*) and transforming growth factor beta receptor 1 (*TGFBR1*), accompanied by an increase in the expression of specific neurodegeneration-associated genes that included C-X-C motif chemokine receptor 4 (*CXCR4*) and glycoprotein NMB (*GPNMB*), in the diseased group (Fig. 6A). Expression of *SNCA* and leucine-rich repeat kinase 2 (*LRRK2*) with known genetic association to Parkinson's disease was also significantly elevated in microglia from Parkinson's disease/Lewy body dementia patients

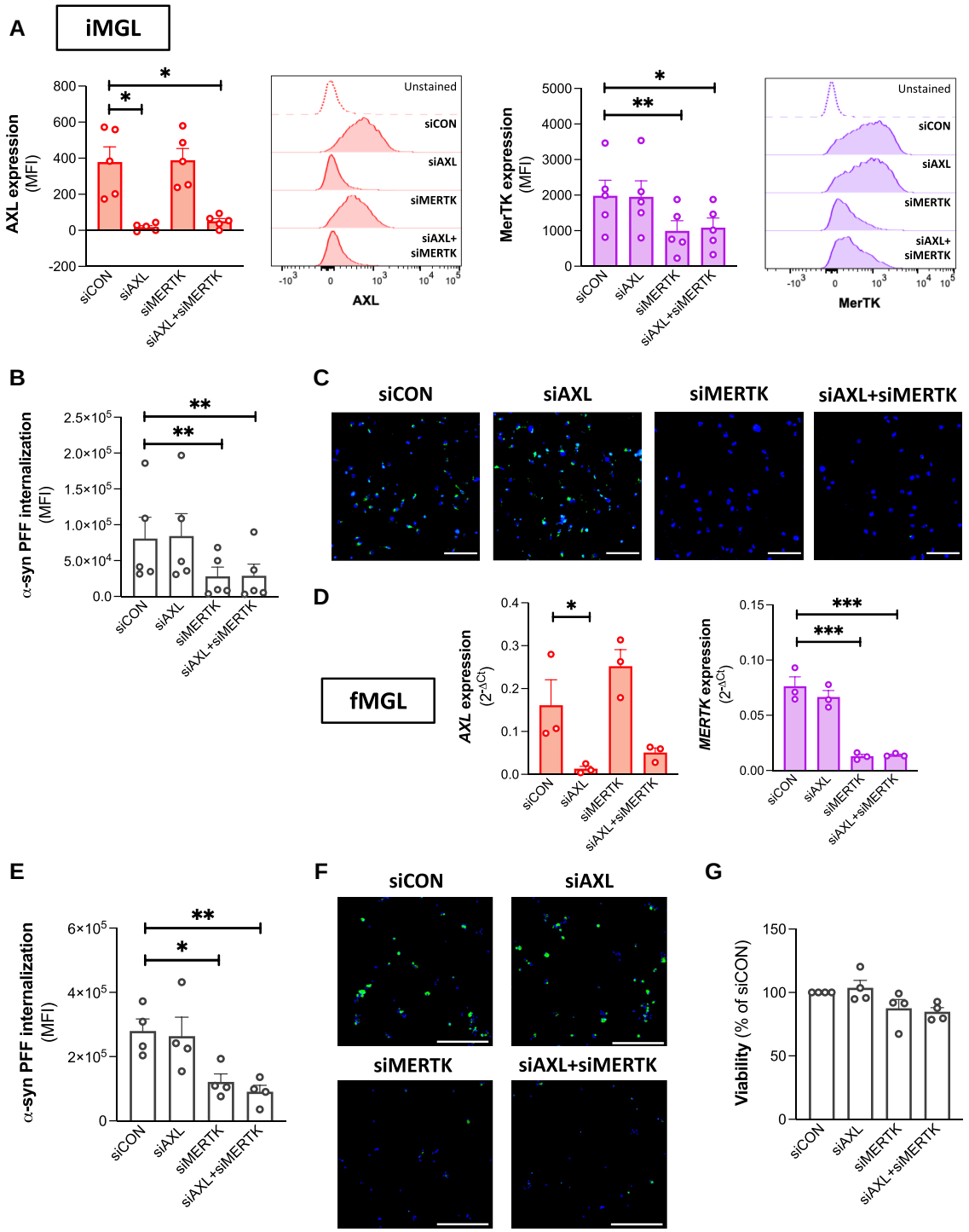

Figure 4 Effect of *AXL*/*MERTK* knockdown on microglial uptake of α-synuclein preformed fibrils. Microglia were transfected with siCON, siAXL and/or siMERTK. (**A**) Cell surface expression of AXL and MerTK assessed by flow cytometry on live induced pluripotent stem cell-derived microglia (iMGL) 48 h following transfection. Repeated measure one-way ANOVA were performed followed by Dunnett's *post hoc* test. Mean ± SEM of $n = 5$; $^{*}P < 0.05$, $^{**}P < 0.01$; MFI = median fluorescence intensity. (**B**) Quantification of mean green fluorescence intensity (MFI) in induced pluripotent stem cell-derived microglia (iMGL) culture challenged with pHrodo™ Green-labelled α-synuclein (α-syn) preformed fibrils (PFFs) for 2 h. A repeated measure one-way ANOVA was performed followed by Dunnett's *post hoc* test. Mean ± SEM of $n = 5$; $^{**}P < 0.01$. (**C**) Representative images of iMGL challenged with pHrodo™ Green-labelled α-syn PFFs for 2 h and counterstained with Hoechst 33342 (blue). Scale bar = 150 μm. (**D**) qRT-PCR assessment of *AXL* and *MERTK* expression in fetal microglia (fMGL) 48 h following transfection. Repeated measure one-way ANOVA were performed followed by Dunnett's *post hoc* test. Mean ± SEM of $n = 3$; $^{*}P < 0.05$, $^{***}P < 0.001$. (**E**) Quantification of mean green fluorescence intensity (MFI) in fMGL culture challenged with pHrodo™ Green-labelled α-syn PFFs for 2 h. A repeated measure one-way ANOVA was performed followed by Dunnett's *post hoc* test. Mean ± SEM of $n = 4$; $^{*}P < 0.05$, $^{**}P < 0.01$. (**F**) Representative fluorescence images of fMGL challenged with pHrodo™ Green-labelled α-syn PFFs for 2 h and counterstained with Hoechst 33342 (blue). Scale bar = 200 μm. (**G**) Viability of fMGL 48 h following transfection. A repeated measure one-way ANOVA was performed followed by Dunnett's *post hoc* test. Mean ± SEM of $n = 4$.

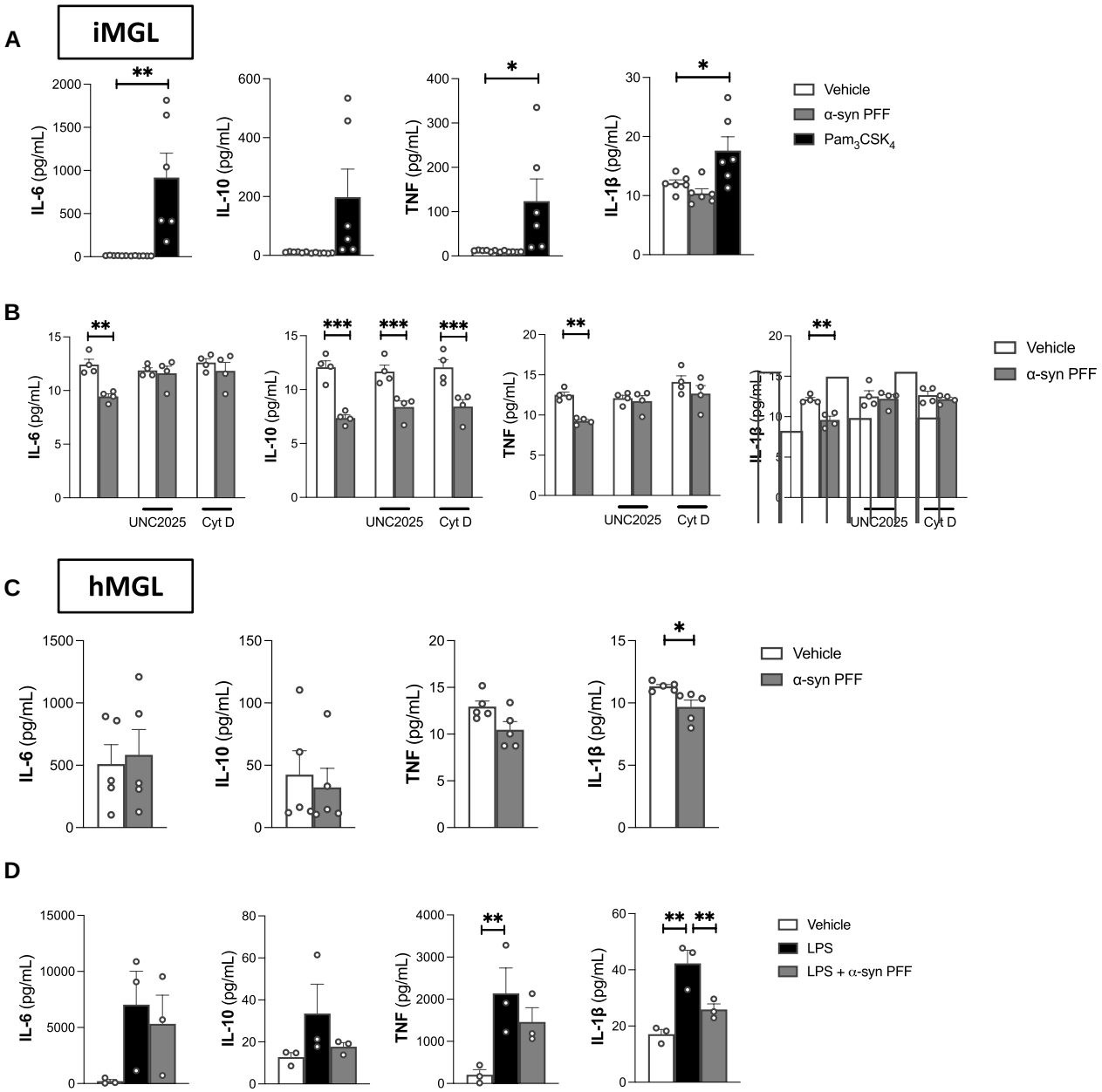

Figure 5 Inflammatory response of human microglia to α-synuclein preformed fibrils. Microglia were treated for 24 h with vehicle, Pam_3CSK_4 (100 ng/ml), lipopolysaccharide (LPS; 100 ng/ml) and/or α-synuclein (α-syn) preformed fibrils (PFFs) (1 μm). (**A**) Cytokine secretion from induced pluripotent stem cell-derived microglia (iMGL). Repeated measure one-way ANOVA were performed followed by Dunnett's *post hoc* test. Mean ± SEM of $n = 6$; $^{*}P < 0.05$, $^{**}P < 0.01$. (**B**) Cytokine secretion from iMGL pretreated or not with UNC2025 (3 μm) or cytochalasin D (cyt D; 1 μm) for 1 h prior to vehicle/α-syn PFF treatment. Repeated measure one-way ANOVA were performed followed by Sidak's *post hoc* test. Mean ± SEM of $n = 4$; $^{**}P < 0.01$, $^{***}P < 0.001$. (**C**) Cytokine secretion from hMGL. Paired *t*-tests were performed. Mean ± SEM of $n = 6$; $^{*}P < 0.05$. (**D**) Cytokine secretion from human primary microglia (hMGL). Repeated measure one-way ANOVA were performed followed by Sidak's *post hoc* test. Mean ± SEM of $n = 3$; $^{**}P < 0.01$. IL-1β = interleukin-1β; IL-6 = interleukin-6; IL-10 = interleukin-10; TNF = tumor necrosis factor.

(Fig. 6A). Consistent with our *in vitro* data, genes encoding inflammatory cytokines did not figure among the DEGs (Supplementary Table 6). Most importantly, evaluation of genes encoding TAM receptors and their activating ligands revealed *MERTK* expression to be modestly higher in microglia from diseased patients compared to controls (fold change = 1.2, $P = 5.08 \times 10^{-21}$; Fig. 6B and Supplementary Table 6). *MERTK* was ubiquitously expressed across all microglia clusters identified in the dataset (Supplementary Fig. 11). Some clusters predominantly composed of microglia from Parkinson's disease/Lewy body dementia patients had particularly high expression of *MERTK* (Clusters 7, 8, 10, 15 and 16; Supplementary Figs 11 and 12). Aside from microglia which had the highest expression of *MERTK*, macrophages, astrocytes and endothelial cells expressed *MERTK* in the substantia nigra (Supplementary Fig. 13). No significant difference in *MERTK* expression was observed between control and Parkinson's disease/Lewy body dementia patients when DEG analysis was carried out on all cell types combined (Supplementary Table 7).

Table 1 Burden analysis of rare variants in Parkinson's disease

Gene	All non-synonymous, P			All functional, P			CADD score ≥20, P		
	UKBB	AMP-PD	Meta-analysis	UKBB	AMP-PD	Meta-analysis	UKBB	AMP-PD	Meta-analysis
AXL	0.84	0.27	0.48	0.83	0.27	0.48	0.45	0.85	0.54
MERTK	0.2	0.92	0.81	0.21	1	0.78	**0.002**	0.67	0.28

Bold text represents statistically significant value ($P < 0.05$). AMP-PD = Accelerating Medicines Partnership-Parkinson's Disease; CADD = combined annotation dependent depletion; UKBB = UK Biobank.

Analysis of transcriptional changes following *in vitro* exposure of iMGL to α-syn PFFs revealed increased *CXCR4* and *GPNMB* expression after 1 and 7 days, respectively (Supplementary Fig. 10). In contrast, expression of homeostatic markers such as *CX3CR1* and *TGFBR1*, as well as *MERTK* were unaffected by *in vitro* α-syn PFF exposure (Supplementary Fig. 10), suggesting α-syn fibrils are direct drivers of some, but not all, microglial transcriptomic changes in late-stage Parkinson's disease/Lewy body dementia. Transcriptional changes in patient microglia could be a consequence of other processes such as neuronal dysfunction or degeneration.

Upregulation of MerTK protein expression in synucleinopathies was next verified by western blotting using substantia nigra tissues from nine Lewy body dementia patients and nine control donors. Significantly higher amounts of α-syn phosphorylated at serine 129 (S129p), an indicator of α-syn fibril accumulation, but not total α-syn, were detected in substantia nigra lysates of Lewy body dementia patients compared to controls (Fig. 6C and D and Supplementary Fig. 14). This is consistent with previous observations.[54,55] The accumulation of α-syn S129p was unaccompanied by upregulation in MerTK protein expression in whole tissue lysates (Fig. 6C and D). Similar observations were made using cortex tissues from five Lewy body dementia patients and five non-neurological control donors (Fig. 6E and F and Supplementary Fig. 15). Altogether, the data suggest a lack of substantial upregulation in MerTK expression in synucleinopathies such as Lewy body dementia.

Discussion

In summary, our study identified MerTK as an essential receptor that mediates α-syn fibril uptake by human microglia. Using orthogonal assays, including pharmacological inhibition of MerTK kinase activity, *MERTK* downregulation induced by phenotypic polarization and *MERTK* knockdown by siRNA, we show that α-syn fibril internalization by human microglia is dependent on MerTK. MerTK-mediated internalization of α-syn PFFs was not observed to induce the expression and secretion of inflammatory cytokines. Moreover, *MERTK* mRNA expression was found to be only modestly increased in microglia from Parkinson's disease/Lewy body dementia patients compared to control donors. At the whole tissue level, accumulation of α-syn S129p in the brains of Lewy body dementia patients was unaccompanied by MerTK protein upregulation. *MERTK* mRNA upregulation in microglia might not have translated into higher protein expression, or was too modest to be reflected at the tissue level given that other cell types such as astrocyte express MerTK. Our data exclude the possibility that a dysregulated MerTK pathway is responsible for α-syn fibril accumulation in Parkinson's disease/Lewy body dementia, since no downregulation of MerTK expression was observed. However, specific genetic variants that are deleterious to MerTK function could be associated with Parkinson's disease according to the result of our burden analysis. Overall, our findings imply that therapeutic upregulation of this pathway in synucleinopathies might promote α-syn fibril clearance without inducing inflammation.

Phagocytosis of cellular debris is a complex process that involves multiple cell surface proteins, some mediating tethering of the target and some initiating engulfment through cytoskeletal remodelling. Pattern recognition receptors such as TLRs can come into contact with their agonistic motifs during this process and trigger an inflammatory response.[56] α-Syn has been repeatedly observed to induce inflammatory cytokine release from murine microglia,[16-20] albeit with some contradictory findings.[57] With regards to human iMGL, Trudler *et al.*[58] previously observed inflammasome activation and IL-1β secretion following cell treatment with non-sonicated large size α-syn PFFs (>2000 nm), whereas Rostami *et al.*[14] failed to observe IL-1β secretion from iMGL following sonicated, smaller α-syn PFFs treatment. With regards to hMGL, non-sonicated α-syn PFFs were previously shown by Pike *et al.*[59] to induce inflammasome activation and subsequent IL-1β release from hMGL. In our study, α-syn PFFs sonicated to ∼50–100 nm in size were employed because of the demonstrated pathogenicity and propensity for propagation of smaller PFFs.[60,61] These small PFFs were actively phagocytosed but failed to induce IL-1β secretion from hMGL or iMGL. Notably, microglia in both the Pike *et al.*[59] and Trudler *et al.*[58] studies were cultured in the presence of granulocyte-macrophage colony-stimulating factor (GM-CSF), which might have influenced microglia response to α-syn PFFs. Finally, Pike *et al.*[59] used saturating concentrations of α-syn PFFs (5–20 μM), which might have resulted in stress-induced non-specific activation of microglia.

Although the TAM receptors AXL and MerTK were thought to have redundant roles in phagocytosis, MerTK but not AXL has been demonstrated to mediate homeostatic phagocytosis. Daily clearance of photoreceptor outer segments by retinal pigment epithelial cells in the retina and apoptotic germ cells by Sertoli cells in the testis are mediated by MerTK,[62] without which accumulation of cellular debris leads to tissue degeneration.[29,63-65] AXL and MerTK expression are also differentially regulated by tolerogenic and inflammatory stimuli: whereas MerTK expression is increased by treatment with glucocorticoids, AXL is upregulated and MerTK downmodulated following lipopolysaccharide or polyinosinic:polycytidylic treatment of macrophages.[66,67] Here, we observed that microglial uptake of α-syn fibrils is dependent on MerTK but not AXL despite both receptors being expressed by human microglia. Consistent with the *in vitro* observations, only *MERTK* but not *AXL* variants were genetically associated with Parkinson's disease cases in the UKBB cohort.

In a study that quantified the presence of α-syn inclusions in different cell types of the olfactory bulb of Parkinson's disease patients, ∼8% of microglia have been shown to contain inclusions, a strikingly high percentage considering that ∼9% of neurons were found to contain inclusions in the same study.[68] The main source of microglia-internalized α-syn in the Parkinson's disease brain remains unclear. α-Syn has been detected in the cerebrospinal fluid

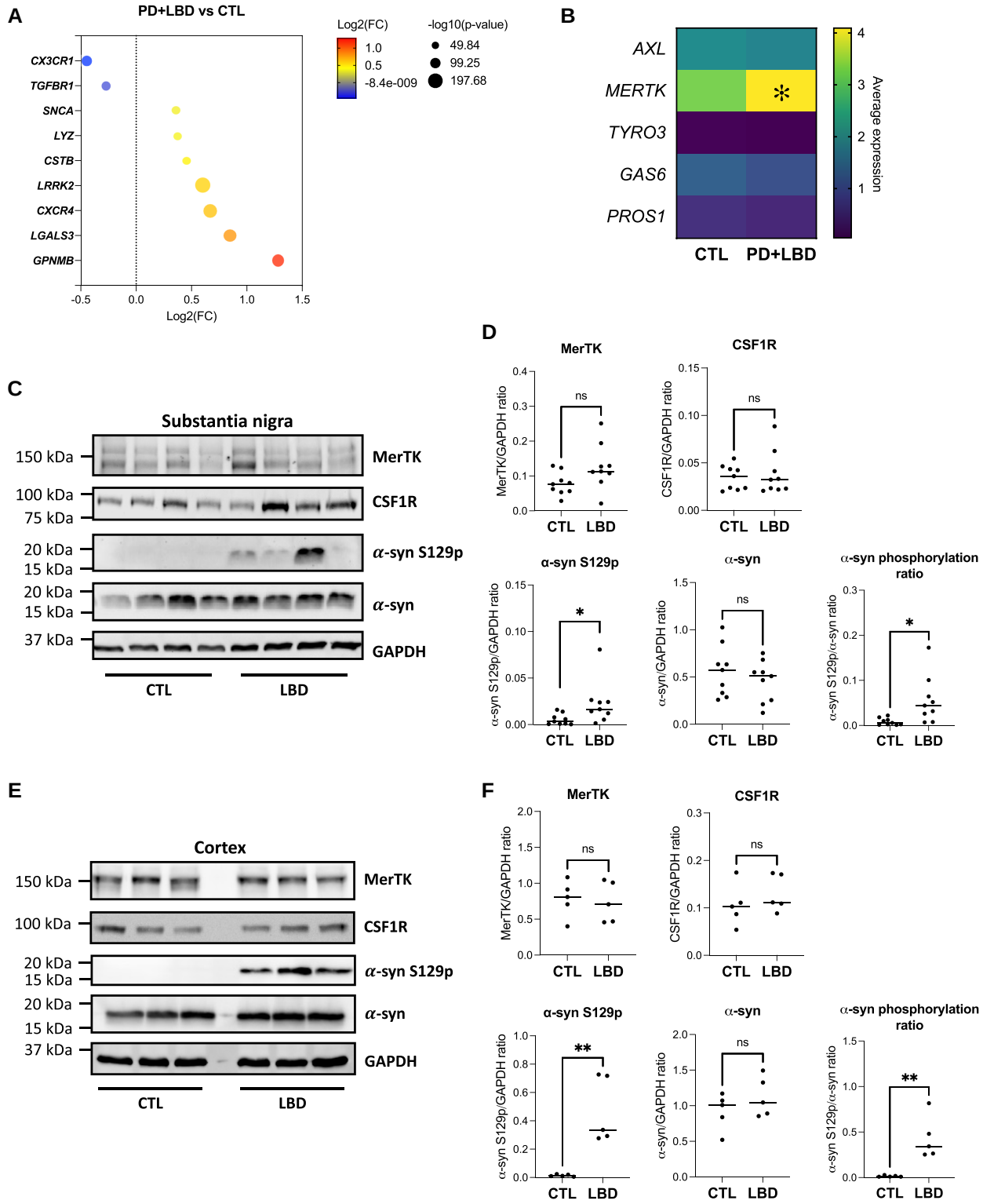

Figure 6 MerTK expression in Parkinson's disease and Lewy body dementia. (**A** and **B**) Single-nuclei RNA-sequencing data from Kamath *et al.*[47] were used to compare microglia from substantia nigra of seven Parkinson's disease (PD) patients and three Lewy body dementia (LBD) patients versus eight control (CTL) donors. (**A**) Dot plot depicting examples of identified differentially expressed genes (DEGs) between PD + LBD and CTL. (**B**) Heatmap showing the average expression of genes encoding TAM receptors and their activating ligands. $^{*}P < 0.05$ in DEG analysis. (**C** and **D**) Western blotting using human substantia nigra tissues of LBD and CTL donors. (**C**) Representative blots. Proteins were extracted in the presence of SDS and urea to solubilize α-synuclein (α-syn) aggregates. (**D**) Quantification of MerTK, CSF1R, phosphorylated α-syn (S129p) and α-syn expression. Mann–Whitney tests were performed; $n = 9$; ns = non-significant; $^{*}P < 0.05$. (**E** and **F**) Western blotting using human cortex of LBD and CTL donors. (**E**) Representative blots. Proteins were extracted in the presence of SDS and urea to solubilize α-syn aggregates. (**F**) Quantification of MerTK, CSF1R, phosphorylated α-syn (S129p) and α-syn expression. Mann–Whitney tests were performed; $n = 5$; ns = non-significant; $^{**}P < 0.01$.

and brain interstitial fluid, suggesting the protein is released by neurons into the extracellular space through secretion or cell death.[69,70] The current study therefore focused on the role of MerTK in internalization of extracellular α-syn fibrils. However, MerTK could well be mediating α-syn internalization through phagocytosis of synapses[71] and apoptotic neurons,[72] limiting neuronal spread of α-syn.

MerTK has been receiving increasing attention as a potential therapeutic target in proteinopathies over recent years. In the APP/PS1 mouse model of Alzheimer's disease, Axl and MerTK have been shown to be important for microglia migration to amyloid plaques.[73] Genetic ablation of *Axl* and/or *Mertk* led to accelerated death of the animals,[74] indicating a protective role for these receptors against disease progression. Longitudinal studies revealed that higher circulating levels of cleaved, soluble TAM receptors and their ligand GAS6 in the CSF are associated with better cognitive outcome in Alzheimer's disease.[75,76] To our knowledge, the current study represents the first *in vitro* demonstration of MerTK involvement in protein aggregate internalization. Pharmacological targeting of MerTK is difficult because of its wide expression and pleiotropic roles. Enhancement of MerTK expression or function in the brain is likely to increase phagocytosis of all MerTK targets, including myelin, synapses, apoptotic cells and even live neurons in a process termed phagoptosis.[77] Bispecific antibodies and hybrid proteins with affinities to both MerTK and amyloid beta have been designed to specifically target amyloid beta to MerTK-mediated, non-inflammatory phagocytosis in Alzheimer's disease.[78,79] Similar strategies could be adopted to selectively enhance α-syn clearance through MerTK in synucleinopathies.

In conclusion, we report for the first time a role for MerTK in the uptake of α-syn fibrils by human microglia. This pathway could be leveraged to promote α-syn fibril clearance in synucleinopathies such as Parkinson's disease without inducing an inflammatory response from microglia.

Data availability

RNAseq data from Dorion *et al.*[25] are available through Gene Expression Omnibus (GSE228755). snRNAseq data from Kamath *et al.*[47] are available through the Gene Expression Omnibus (GSE178265).

Acknowledgements

We thank lab members Manon Blain, Qiao-Ling Cui, Genevieve Dorval, Andrea Krahn, Wolfgang Reintsch, Julien Sirois and Vincent Soubannier for technical or administrative assistance. We thank BDRL members Kimberly A. Aldinger, Dan Doherty, Ian G. Phelps, Jennifer C. Dempsey, Kevin J. Lee and Lucinda A. Cort. We would like to thank the participants in the different cohorts for contributing to this study. This research used the NeuroHub infrastructure and was undertaken thanks in part to funding from the Canada First Research Excellence Fund, awarded through the Healthy Brains for Healthy Lives (HBHL) initiative at McGill University, Calcul Québec and Compute Canada. UKBB Resources were accessed under application number 45551. Data used in the preparation of this article were obtained from the AMP PD Knowledge Platform. For up-to-date information on the study, visit https://www.amp-pd.org. AMP PD—a public-private partnership—is managed by the FNIH and funded by Celgene, GSK, the Michael J. Fox Foundation for Parkinson's Research (MJFF), the National Institute of Neurological Disorders and Stroke, Pfizer, Sanofi and Verily. Genetic data used in preparation of this article were obtained from the Fox Investigation for New Discovery of Biomarkers (BioFIND), the Harvard Biomarker Study (HBS), the Parkinson's Progression Markers Initiative (PPMI), the Parkinson's Disease Biomarkers Program (PDBP), the International LBD Genomics Consortium (iLBDGC) and the STEADY-PD III Investigators. BioFIND is sponsored by MJFF with support from the National Institute for Neurological Disorders and Stroke (NINDS). The BioFIND Investigators have not participated in reviewing the data analysis or content of the manuscript. For up-to-date information on the study, visit michaeljfox.org/news/biofind. The HBS is a collaboration of HBS investigators (Co-Directors: Brigham and Women's Hospital: Clemens R. Scherzer, Massachusetts General Hospital: Bradley T. Hyman; Investigators and Study Coordinators: Brigham and Women's Hospital: Yuliya Kuras, Karbi Choudhury, Michael T. Hayes, Aleksandar Videnovic, Nutan Sharma, Vikram Khurana, Claudio Melo De Gusmao, Reisa Sperling; Massachusetts General Hospital: John H. Growdon, Michael A. Schwarzschild, Albert Y. Hung, Alice W. Flaherty, Deborah Blacker, Anne-Marie Wills, Steven E. Arnold, Ann L. Hunt, Nicte I. Mejia, Anand Viswanathan, Stephen N. Gomperts, Mark W. Albers, Maria Allora-Palli, David Hsu, Alexandra Kimball, Scott McGinnis, John Becker, Randy Buckner, Thomas Byrne, Maura Copeland, Bradford Dickerson, Matthew Frosch, Theresa Gomez-Isla, Steven Greenberg, Julius Hedden, Elizabeth Hedley-Whyte, Keith Johnson, Raymond Kelleher, Aaron Koenig, Maria Marquis-Sayagues, Gad Marshall, Sergi Martinez-Ramirez, Donald McLaren, Olivia Okereke, Elena Ratti, Christopher William, Koene Van Dij, Shuko Takeda, Anat Stemmer-Rachaminov, Jessica Kloppenburg, Catherine Munro, Rachel Schmid, Sarah Wigman, Sara Wlodarcsyk; Data Coordination: Brigham and Women's Hospital: Thomas Yi; Biobank Management Staff: Brigham and Women's Hospital: Idil Tuncali.) and funded through philanthropy and National Institutes of Health (NIH) and Non-NIH funding sources. The HBS Investigators have not participated in reviewing the data analysis or content of the manuscript. PPMI—a public-private partnership—is funded by MJFF and funding partners, including 4D Pharma, AbbVie Inc., AcureX Therapeutics, Allergan, Amathus Therapeutics, Aligning Science Across Parkinson's (ASAP), Avid Radiopharmaceuticals, Bial Biotech, Biogen, BioLegend, Bristol Myers Squibb, Calico Life Sciences LLC, Celgene Corporation, DaCapo Brainscience, Denali Therapeutics, The Edmond J. Safra Foundation, Eli Lilly and Company, GE Healthcare, GSK, Golub Capital, Handl Therapeutics, Insitro, Janssen Pharmaceuticals, Lundbeck, Merck & Co., Inc., Meso Scale Diagnostics, LLC, MJFF, Neurocrine Biosciences, Pfizer Inc., Piramal Imaging, Prevail Therapeutics, F. Hoffmann-La Roche Ltd and its affiliated company Genentech Inc., Sanofi Genzyme, Servier, Takeda Pharmaceutical Company, Teva Neuroscience, Inc., UCB, Vanqua Bio, Verily Life Sciences, Voyager Therapeutics, Inc., Yumanity Therapeutics, Inc. The PPMI Investigators have not participated in reviewing the data analysis or content of the manuscript. For up-to-date information on the study, visit www.ppmi-info.org. The PDBP consortium is supported by the NINDS at the National Institutes of Health. A full list of PDBP investigators can be found at https://pdbp.ninds.nih.gov/policy. The PDBP investigators have not participated in reviewing the data analysis or content of the manuscript. Genome Sequencing in Lewy Body Dementia and Neurologically Healthy Controls: A Resource for the Research Community was generated

by the iLBDGC, under the co-directorship by Dr. Bryan J. Traynor and Dr. Sonja W. Scholz from the Intramural Research Program of the U.S. National Institutes of Health. The iLBDGC Investigators have not participated in reviewing the data analysis or content of the manuscript. For a complete list of contributors, please see: https://doi.org/10.1101/2020.07.06.185066. STEADY-PD III is a 36-month, Phase 3, parallel group, placebo-controlled study of the efficacy of isradipine 10 mg daily in 336 participants with early Parkinson's disease that was funded by the NINDS and supported by MJFF and the Parkinson's Study Group. The STEADY-PD III Investigators have not participated in reviewing the data analysis or content of the manuscript. The full list of STEADY PD III investigators can be found at: https://clinicaltrials.gov/ct2/show/NCT02168842.

Funding

M.-F.D. is supported by a scholarship from the Canadian Institutes of Health Research. K.S. is supported by a post-doctoral fellowship from the Canada First Research Excellence Fund, awarded to McGill University as part of the Healthy Brains, Healthy Lives initiative, and Fonds de Recherche du Québec -Santé post-doctoral fellowship. I.A.G. and the BDRL was supported by National Institutes of Health award number 5R24HD000836 from the Eunice Kennedy Shriver National Institute of Child Health and Human Development. E.A.F. is supported by a Canadian Institutes of Health Research foundation grant (FDN-154301), a Fonds d'Accéleration des Collaborations en Santé grant from Consortium Québécois sur la Découverte du Médicament/Ministère de l'Économie et de l'Innovation (CQDM/MEI) and by a Canada Research Chair (Tier 1) in Parkinson's disease. Z.G.O. is supported by the Fonds de Recherche du Quebéc - Santé Chercheurs-boursiers award, in collaboration with Parkinson Québec, and is a William Dawson Scholar. T.M.D. was supported by the Canada First Research Excellence Fund, awarded through the Healthy Brains, Healthy Lives initiative at McGill University, the Health Collaborations Accelerator Fund program and Quantum Leaps program of Consortium Québécois sur la Découverte du Médicament, the Sebastian and Ghislaine van Berkom Foundation, the Alain and Sandra Bouchard Foundation and a project grant from Canadian Institutes of Health Research (PJT—169095).

Competing interests

The authors report no competing interests.

Supplementary material

Supplementary material is available at *Brain* online.

References

1. Klein C, Westenberger A. Genetics of Parkinson's disease. *Cold Spring Harb Perspect Med*. 2012;2:a008888.
2. Braak H, Rüb U, Gai WP, Del Tredici K. Idiopathic Parkinson's disease: Possible routes by which vulnerable neuronal types may be subject to neuroinvasion by an unknown pathogen. *J Neural Transm (Vienna)*. 2003;110:517-536.
3. Surmeier DJ, Obeso JA, Halliday GM. Selective neuronal vulnerability in Parkinson disease. *Nat Rev Neurosci*. 2017;18:101-113.
4. Challis C, Hori A, Sampson TR, *et al*. Gut-seeded α-synuclein fibrils promote gut dysfunction and brain pathology specifically in aged mice. *Nat Neurosci*. 2020;23:327-336.
5. Recasens A, Dehay B, Bové J, *et al*. Lewy Body extracts from Parkinson disease brains trigger α-synuclein pathology and neurodegeneration in mice and monkeys. *Ann Neurol*. 2014;75:351-362.
6. Borghammer P, Van Den Berge N. Brain-first versus gut-first Parkinson's disease: A hypothesis. *J Parkinsons Dis*. 2019;9(s2):S281-s295.
7. Prusiner SB, Woerman AL, Mordes DA, *et al*. Evidence for α-synuclein prions causing multiple system atrophy in humans with parkinsonism. *Proc Natl Acad Sci U S A*. 2015;112:E5308-E5317.
8. Polinski NK. A summary of phenotypes observed in the in vivo rodent alpha-synuclein preformed fibril model. *J Parkinsons Dis*. 2021;11:1555-1567.
9. Mahul-Mellier A-L, Burtscher J, Maharjan N, *et al*. The process of Lewy body formation, rather than simply α-synuclein fibrillization, is one of the major drivers of neurodegeneration. *Proc Natl Acad Sci U S A*. 2020;117:4971-4982.
10. Volpicelli-Daley LA, Luk KC, Patel TP, *et al*. Exogenous α-synuclein fibrils induce Lewy body pathology leading to synaptic dysfunction and neuron death. *Neuron*. 2011;72:57-71.
11. Castonguay AM, Gravel C, Lévesque M. Treating Parkinson's disease with antibodies: Previous studies and future directions. *J Parkinsons Dis*. 2021;11:71-92.
12. Ihse E, Yamakado H, van Wijk XM, Lawrence R, Esko JD, Masliah E. Cellular internalization of alpha-synuclein aggregates by cell surface heparan sulfate depends on aggregate conformation and cell type. *Sci Rep*. 2017;7:9008.
13. Scheiblich H, Dansokho C, Mercan D, *et al*. Microglia jointly degrade fibrillar alpha-synuclein cargo by distribution through tunneling nanotubes. *Cell Sep*. 2021;184:5089-5106.e21.
14. Rostami J, Mothes T, Kolahdouzan M, *et al*. Crosstalk between astrocytes and microglia results in increased degradation of α-synuclein and amyloid-β aggregates. *J Neuroinflammation*. 2021;18:124.
15. Lee H-J, Suk J-E, Bae E-J, Lee S-J. Clearance and deposition of extracellular α-synuclein aggregates in microglia. *Biochem Biophys Res Commun*. 2008;372:423-428.
16. Long H, Zhang S, Zeng S, *et al*. Interaction of RAGE with α-synuclein fibrils mediates inflammatory response of microglia. *Cell Rep*. 2022;40:111401.
17. Fellner L, Irschick R, Schanda K, *et al*. Toll-like receptor 4 is required for α-synuclein dependent activation of microglia and astroglia. *Glia*. 2013;61:349-360.
18. Kim C, Ho D-H, Suk J-E, *et al*. Neuron-released oligomeric α-synuclein is an endogenous agonist of TLR2 for paracrine activation of microglia. *Nat Commun*. 2013;4:1562.
19. Panicker N, Sarkar S, Harischandra DS, *et al*. Fyn kinase regulates misfolded α-synuclein uptake and NLRP3 inflammasome activation in microglia. *J Exp Med*. 2019;216:1411-1430.
20. Scheiblich H, Bousset L, Schwartz S, *et al*. Microglial NLRP3 inflammasome activation upon TLR2 and TLR5 ligation by distinct α-synuclein assemblies. *J Immunol*. 2021;207:2143-2154.
21. Healy LM, Yaqubi M, Ludwin S, Antel J. Species differences in immune-mediated CNS tissue injury and repair: A (neuro)inflammatory topic. *Glia*. 2020;68:811-829.
22. Geirsdottir L, David E, Keren-Shaul H, *et al*. Cross-species single-cell analysis reveals divergence of the primate microglia program. *Cell*. 2019;179:1609-1622.e16.

23. Gosselin D, Skola D, Coufal NG, *et al*. An environment-dependent transcriptional network specifies human microglia identity. *Science*. 2017;356:eaal3222.
24. Owen DR, Narayan N, Wells L, *et al*. Pro-inflammatory activation of primary microglia and macrophages increases 18 kDa translocator protein expression in rodents but not humans. *J Cereb Blood Flow Metab*. 2017;37:2679-2690.
25. Dorion M-F, Yaqubi M, Murdoch HJ, *et al*. Systematic comparison of culture media uncovers phenotypic shift of primary human microglia defined by reduced reliance to CSF1R signaling. *Glia*. 2023;71:1278-1293.
26. Healy LM, Perron G, Won S-Y, *et al*. MerTK is a functional regulator of myelin phagocytosis by human myeloid cells. *J Immunol*. 2016;196:3375-3384.
27. Scott RS, McMahon EJ, Pop SM, *et al*. Phagocytosis and clearance of apoptotic cells is mediated by MER. *Nature*. 2001;411:207-211.
28. Chung WS, Clarke LE, Wang GX, *et al*. Astrocytes mediate synapse elimination through MEGF10 and MERTK pathways. *Nature*. 2013;504:394-400.
29. D'Cruz PM, Yasumura D, Weir J, *et al*. Mutation of the receptor tyrosine kinase gene Mertk in the retinal dystrophic RCS rat. *Hum Mol Genet*. 2000;9:645-651.
30. Feng W, Yasumura D, Matthes MT, LaVail MM, Vollrath D. Mertk triggers uptake of photoreceptor outer segments during phagocytosis by cultured retinal pigment epithelial cells. *J Biol Chem*. 2002;277:17016-17022.
31. Lemke G. Biology of the TAM receptors. *Cold Spring Harb Perspect Biol*. 2013;5:a009076.
32. Rothlin CV, Carrera-Silva EA, Bosurgi L, Ghosh S. TAM receptor signaling in immune homeostasis. *Annu Rev Immunol*. 2015;33:355-391.
33. Butovsky O, Jedrychowski MP, Moore CS, *et al*. Identification of a unique TGF-β-dependent molecular and functional signature in microglia. *Nat Neurosci*. 2014;17:131-143.
34. Durafourt BA, Moore CS, Blain M, Antel JP. Isolating, culturing, and polarizing primary human adult and fetal microglia. *Methods Mol Biol*. 2013;1041:199-211.
35. Chen CX, Abdian N, Maussion G, *et al*. A multistep workflow to evaluate newly generated iPSCs and their ability to generate different cell types. *Methods Protoc*. 2021;4:50.
36. McQuade A, Coburn M, Tu CH, Hasselmann J, Davtyan H, Blurton-Jones M. Development and validation of a simplified method to generate human microglia from pluripotent stem cells. *Mol Neurodegener*. 2018;13:67.
37. Bourgey M, Dali R, Eveleigh R, *et al*. Genpipes: An open-source framework for distributed and scalable genomic analyses. *Gigascience*. 2019;8:giz037.
38. Sasaki A, Arawaka S, Sato H, Kato T. Sensitive western blotting for detection of endogenous Ser129-phosphorylated α-synuclein in intracellular and extracellular spaces. *Sci Rep*. 2015;5:14211.
39. Maneca D-L, Luo W, Krahn A, *et al*. Production of recombinant α synuclein monomers and preformed fibrils (PFFs) (V3.0). *Zenodo*. 2022; https://doi.org/10.5281/zenodo.6430401
40. Del Cid Pellitero E, Shlaifer R, Luo W, *et al*. Quality control characterization of α-synuclein preformed fibrils (PFFs) (V3.0). *Zenodo*. 2019; https://doi.org/10.5281/zenodo.6524616
41. Healy LM, Jang JH, Won S-Y, *et al*. MerTK-mediated regulation of myelin phagocytosis by macrophages generated from patients with MS. *Neurol Neuroimmunol Neuroinflamm*. 2017;4:e402.
42. Hughes AJ, Daniel SE, Kilford L, Lees AJ. Accuracy of clinical diagnosis of idiopathic Parkinson's disease: A clinico-pathological study of 100 cases. *J Neurol Neurosurg Psychiatry*. 1992;55:181-184.
43. Postuma RB, Berg D, Stern M, *et al*. MDS Clinical diagnostic criteria for Parkinson's disease. *Mov Disord*. 2015;30:1591-1601.
44. Carson AR, Smith EN, Matsui H, *et al*. Effective filtering strategies to improve data quality from population-based whole exome sequencing studies. *BMC Bioinformatics*. 2014;15:125.
45. Zhao Z, Bi W, Zhou W, VandeHaar P, Fritsche LG, Lee S. UK Biobank whole-exome sequence binary phenome analysis with robust region-based rare-variant test. *Am J Hum Genet*. 2020;106:3-12.
46. Lee S, Teslovich TM, Boehnke M, Lin X. General framework for meta-analysis of rare variants in sequencing association studies. *Am J Hum Genet*. 2013;93:42-53.
47. Kamath T, Abdulraouf A, Burris SJ, *et al*. Single-cell genomic profiling of human dopamine neurons identifies a population that selectively degenerates in Parkinson's disease. *Nat Neurosci*. 2022;25:588-595.
48. Miksa M, Komura H, Wu R, Shah KG, Wang P. A novel method to determine the engulfment of apoptotic cells by macrophages using pHrodo succinimidyl ester. *J Immunol Methods*. 2009;342(1–2):71-77.
49. Söderberg O, Gullberg M, Jarvius M, *et al*. Direct observation of individual endogenous protein complexes in situ by proximity ligation. *Nat Methods*. 2006;3:995-1000.
50. Zhang W, DeRyckere D, Hunter D, *et al*. UNC2025, a potent and orally bioavailable MER/FLT3 dual inhibitor. *J Med Chem*. 2014;57:7031-7041.
51. Junker F, Gordon J, Qureshi O. Fc gamma receptors and their role in antigen uptake, presentation, and T cell activation. Review. *Front Immunol*. 2020;11:1393.
52. Henriksen L, Grandal MV, Knudsen SL, van Deurs B, Grøvdal LM. Internalization mechanisms of the epidermal growth factor receptor after activation with different ligands. *PLoS One*. 2013;8:e58148.
53. Lemke G, Rothlin CV. Immunobiology of the TAM receptors. *Nat Rev Immunol*. 2008;8:327-336.
54. Landeck N, Hall H, Ardah MT, *et al*. A novel multiplex assay for simultaneous quantification of total and S129 phosphorylated human alpha-synuclein. *Mol Neurodegener*. 2016;11:61.
55. Moors TE, Mona D, Luehe S, *et al*. Multi-platform quantitation of alpha-synuclein human brain proteoforms suggests disease-specific biochemical profiles of synucleinopathies. *Acta Neuropathol Commun*. 2022;10:82.
56. Underhill DM, Goodridge HS. Information processing during phagocytosis. *Nat Rev Immunol*. 2012;12:492-502.
57. Li N, Stewart T, Sheng L, *et al*. Immunoregulation of microglial polarization: An unrecognized physiological function of α-synuclein. *J Neuroinflammation*. 2020;17:272.
58. Trudler D, Nazor KL, Eisele YS, *et al*. Soluble α-synuclein–antibody complexes activate the NLRP3 inflammasome in hiPSC-derived microglia. *Proc Natl Acad Sci U S A*. 2021;118:e2025847118.
59. Pike AF, Varanita T, Herrebout MAC, *et al*. α-Synuclein evokes NLRP3 inflammasome-mediated IL-1β secretion from primary human microglia. *Glia*. 2021;69:1413-1428.
60. Abdelmotilib H, Maltbie T, Delic V, *et al*. α-Synuclein fibril-induced inclusion spread in rats and mice correlates with dopaminergic neurodegeneration. *Neurobiol Dis*. 2017;105:84-98.
61. Tarutani A, Suzuki G, Shimozawa A, *et al*. The effect of fragmented pathogenic α-synuclein seeds on prion-like propagation. *J Biol Chem*. 2016;291:18675-18688.
62. Lew ED, Oh J, Burrola PG, *et al*. Differential TAM receptor-ligand-phospholipid interactions delimit differential TAM bioactivities. *Elife*. 2014;3:e03385.
63. Burstyn-Cohen T, Lew ED, Través PG, Burrola PG, Hash JC, Lemke G. Genetic dissection of TAM receptor-ligand interaction in retinal pigment epithelial cell phagocytosis. *Neuron*. 2012;76:1123-1132.

64. Duncan JL, LaVail MM, Yasumura D, *et al*. An RCS-like retinal dystrophy phenotype in mer knockout mice. *Invest Ophthalmol Vis Sci*. 2003;44:826-838.
65. Lu Q, Gore M, Zhang Q, *et al*. Tyro-3 family receptors are essential regulators of mammalian spermatogenesis. *Nature*. 1999; 398:723-728.
66. Zagórska A, Través PG, Lew ED, Dransfield I, Lemke G. Diversification of TAM receptor tyrosine kinase function. *Nat Immunol*. 2014;15:920-928.
67. Wanke F, Gutbier S, Rümmelin A, *et al*. Ligand-dependent kinase activity of MERTK drives efferocytosis in human iPSC-derived macrophages. *Cell Death Dis*. 2021;12:538.
68. Stevenson TJ, Murray HC, Turner C, Faull RLM, Dieriks BV, Curtis MA. α-Synuclein inclusions are abundant in non-neuronal cells in the anterior olfactory nucleus of the Parkinson's disease olfactory bulb. *Sci Rep*. 2020;10:6682.
69. Emmanouilidou E, Elenis D, Papasilekas T, *et al*. Assessment of α-synuclein secretion in mouse and human brain parenchyma. *PLoS One*. 2011;6:e22225.
70. Yamada K, Iwatsubo T. Extracellular α-synuclein levels are regulated by neuronal activity. *Mol Neurodegener*. 2018;13:9.
71. Park J, Choi Y, Jung E, Lee SH, Sohn JW, Chung WS. Microglial MERTK eliminates phosphatidylserine-displaying inhibitory post-synapses. *EMBO J*. 2021;40:e107121.
72. Damisah EC, Hill RA, Rai A, *et al*. Astrocytes and microglia play orchestrated roles and respect phagocytic territories during neuronal corpse removal in vivo. *Sci Adv*. 2020;6:eaba3239.
73. Huang Y, Happonen KE, Burrola PG, *et al*. Microglia use TAM receptors to detect and engulf amyloid β plaques. *Nat Immunol*. 2021;22:586-594.
74. Huang Y, Lemke G. Early death in a mouse model of Alzheimer's disease exacerbated by microglial loss of TAM receptor signaling. *Proc Natl Acad Sci U S A*. 2022;119:e2204306119.
75. Pereira JB, Janelidze S, Strandberg O, *et al*. Microglial activation protects against accumulation of tau aggregates in nondemented individuals with underlying Alzheimer's disease pathology. *Nat Aging*. 2022;2:1138-1144.
76. Brosseron F, Maass A, Kleineidam L, *et al*. Soluble TAM receptors sAXL and sTyro3 predict structural and functional protection in Alzheimer's disease. *Neuron*. 2022;110:1009-1022.e4.
77. Brown GC, Neher JJ. Eaten alive! cell death by primary phagocytosis: 'phagoptosis'. *Trends Biochem Sci*. 2012;37:325-332.
78. Kedage V, Ellerman D, Chen Y, *et al*. Harnessing MerTK agonism for targeted therapeutics. *MAbs*. 2020;12:1685832.
79. Samentar LP, Salazar A, Pan P-P, *et al*. A novel hybrid protein promotes Aβ clearance and reduces inflammatory response through MerTK. *bioRxiv*. [Preprint] doi:10.1101/2021.11.03.467048